# RAS mutation-specific signaling dynamics in response to paralog- and state- selective RAS inhibitors

Beau Baars[1], Ana Orive Ramos[1], Ziyue Kou[1], Bijaya Gaire[1], Mathieu Desaunay[1], Christos Adamopoulos[1], Stuart A. Aaronson[1], Shaomeng Wang[2], Poulikos I. Poulikakos[1*]

1. The Tisch Cancer Institute, Department of Oncological Sciences, Icahn School of Medicine at Mount Sinai, New York, New York, United States
2. Rogel Cancer Center, Department of Internal Medicine, Department of Pharmacology, and Department of Medicinal Chemistry, University of Michigan, Ann Arbor, Michigan, United States

* Correspondence to poulikos.poulikakos@mssm.edu

## Main points

**PanRAS(OFF) inhibitors have limited SII and effectiveness.** The Signaling Inhibition Index (SII) – i.e. the differential inhibition of oncogenic signaling between tumor and normal cells - was neutral or negative for panRAS-OFF inhibitors, with comparable or reduced MAPK suppression in KRAS(G12X) mutant versus RAS(WT) cells. KRAS(G13D) models showed reduced sensitivity, particularly with NF1 loss. SHP2+MEK inhibitor combinations also had low SII, with RAS(Q61X) models demonstrating resistance due to NRAS(Q61X) reactivation and impaired SHP2 inhibitor binding.

**PanKRAS(OFF) selective inhibitors have higher SII than panRAS(OFF) inhibitors.** panKRAS(OFF)- selective inhibitors have a higher SII compared to panRAS(OFF) inhibitors, offering better tumor-versus-normal cell selectivity.

**PanRAS(ON) inhibitors have broad but modest SII.** While panRAS(ON) inhibitors displayed a broader activity profile, their ability to selectively inhibit mutant RAS signaling over normal cells remained relatively narrow (low SII).

**Most KRAS-mutant tumors will be insensitive to any single RAS-targeted inhibitor.** State- and paralog-selective inhibitors have enhanced activity in the same RAS-MUT cancer models that are also sensitive to RAS-MUT-specific inhibitors, suggesting that most KRAS-MUT tumors will not respond uniformly to any one RAS-targeting inhibitor.

**SII varies across RAS inhibitors, necessitating tailored therapeutic strategies.** The effectiveness of paralog- and state-selective inhibitors depends on specific RAS mutations and cell context, highlighting the need to integrate SII considerations into the development and clinical application of RAS-targeted therapies.

**Abstract**

A high therapeutic index (TI), balancing potent oncogenic signaling inhibition in tumor cells with minimal effects on normal cells, is critical for effective cancer therapies. Recent advances have introduced diverse RAS-targeting inhibitors, including mutant-specific inhibitors (e.g., KRAS(G12C) and KRAS(G12D)), as well as paralog- and state-selective inhibitors. These include panRAS(OFF) inhibitors targeting inactive RAS, KRAS-selective inhibitors sparing NRAS and HRAS, and panRAS(ON) inhibitors targeting active RAS. However, the signaling inhibition index (SII)—the differential inhibition of oncogenic signaling between RAS-mutant (RAS-MUT) and normal cells—remains poorly defined for these approaches.

In this study, we evaluated the SII of state- and paralog-selective RAS inhibitors across diverse RAS-MUT and RAS-wild-type (RAS-WT) models. PanRAS(OFF) inhibitors exhibited neutral or negative SII, with comparable or reduced MAPK suppression in KRAS(G12X) mutant cells relative to RAS(WT) cells. KRAS(G13D) models showed low sensitivity (negative SII) to panRAS(OFF) inhibitors, particularly in the context of NF1 loss. Combination treatments with SHP2 and MEK inhibitors resulted in low SII, as pathway suppression was similar in RAS-MUT and RAS-WT cells. Furthermore, RAS(Q61X) models were resistant to combined SHP2i+MEKi due to dual mechanisms: MEK inhibitor–induced NRAS(Q61X) reactivation and RAS-MUT-induced SHP2 conformations impairing inhibitor binding.

Overall, panRAS(OFF) inhibitors exhibited the lowest SII. panKRAS(OFF)-selective inhibitors demonstrated a higher SII, while panRAS(ON) inhibitors displayed broader activity but relatively narrow SII. We observed that tumors that were sensitive to RAS-MUT specific inhibitors, were also sensitive to the state-selective RAS inhibitors (OFF, or ON). In fact, all RAS inhibitors (mutant-specific and state or paralog selective) were active in the same portion of RAS-MUT cancers, while the majority were insensitive to all of them. These findings reveal significant SII variability among RAS-targeted inhibitors, depending on the specific RAS driver mutation and cell context. These insights underscore the importance of incorporating SII considerations into the design and clinical application of RAS-targeted therapies to improve therapeutic outcomes.

## Introduction

The RAS family (KRAS, NRAS, and HRAS) of small GTPases regulates MAPK signaling and other downstream effectors by cycling between GTP-bound (active, ON) and GDP-bound (inactive, OFF) states[1,2]. Under normal conditions, RAS signaling is tightly regulated and essential for cell proliferation, differentiation, and survival. This regulation depends on the coordinated activity of Guanine Exchange

Factors (GEFs), such as SOS, which promote GTP loading, and GTPase-Activating Proteins (GAPs), such as NF1, which facilitate GTP hydrolysis. Activated RAS recruits RAF to the membrane for activation of the kinase cascade RAF/MEK/ERK. Activated ERK promotes a transcriptional program that drives cell cycle progression. RAS proteins are frequently mutated in human cancer[1-3], with most common mutations occurring in positions G12, G13 and Q61[1,3]. These mutations shift the steady-state equilibrium in cells towards the RAS-ON state to varying degrees, driving uncontrolled cell proliferation and tumorigenesis[1,3].

Despite being discovered over four decades ago, RAS-MUT has historically been considered "undruggable" due to the lack of well-defined binding pockets for small molecules[4]. However, pioneering work by the Shokat group[5], led to the development of the first direct inhibitors targeting KRAS(G12C), exploiting a druggable pocket in its inactive (GDP-bound) state. This breakthrough has spurred the development of numerous small-molecule inhibitors targeting KRAS(G12C)[6-9], and more recently, KRAS(G12D)[10].

Contrary to the long-held belief that RAS-MUT are "locked" in the active (GTP-bound) state, recent studies[11-14], including our own[15], have demonstrated that RAS(G12X) mutants exist in a dynamic equilibrium between the GTP-bound (ON) and GDP-bound (OFF) states. This discovery has expanded the therapeutic potential of small molecules targeting the inactive conformation (panRAS(OFF) inhibitors, panRAS(OFF)i), including SHP2[11,13-16] and SOS1[17] inhibitors, as well as panKRAS(OFF)-selective compounds that spare NRAS and HRAS[18].

Recent advancements have also led to the development of tricomplex inhibitors, such as panRAS(ON) inhibitors (panRAS(ON)i) (e.g. RMC-7977, ERAS-0015, GFH547), which bind Cyclophilin A (CYPA) to form a high-affinity complex that sterically occludes RAS–effector interactions. This approach enables the targeting of active RAS, a previously inaccessible conformation, and has shown promise across a broad spectrum of RAS-MUT[19,20]. One such compound, RMC-6236, is currently in Phase I clinical trials (NCT05379985).

Despite these advancements, achieving a high Therapeutic Index (TI) remains a significant challenge in RAS/MAPK-targeted therapies. The Signaling Inhibition Index (SII), defined as the ratio of signaling inhibition in tumor versus normal cells, is a critical determinant of TI. While RAS mutant-specific inhibitors offer a theoretically unlimited SI, the SI of paralog- and state-selective inhibitors remains poorly understood. In this study, we aimed to determine and compare the SI of state- and paralog-selective RAS

inhibitors by evaluating signaling dynamics and tumor responses in both RAS-mutant and RAS wild-type (WT) models.

**KRAS(G12X)-expressing cells exhibit differential sensitivity to panRAS(OFF)i.**

Therapeutic strategies targeting oncogenic RAS have traditionally focused on inhibiting downstream effectors, such as MEK, rather than directly targeting RAS itself. The development of mutant-selective KRAS(G12C) inhibitors revealed that certain KRAS mutations remain dependent on RTK-driven GEF activity, opening the possibility of targeting mutant RAS by inhibiting its upstream activators, such as SHP2 or SOS1.

To assess the sensitivity of different KRAS mutations at codon G12 to panRAS(OFF)i, we utilized isogenic HeLa cells engineered with doxycycline (dox)-inducible expression of KRAS(G12C), KRAS(G12D), KRAS(G12A), KRAS(G12S), and KRAS(G12V) (**Fig. 1A**). SHP2 inhibition (SHP2i) was most potent against KRAS(G12C), KRAS(G12A) and KRAS(G12S), consistent with our previous findings[15] and other reports[11-13]. However, SHP2i exhibited reduced activity in KRAS(G12D)- and KRAS(G12V)-expressing cells. Of note, SHP2i led to greater MAPK inhibition in wild-type KRAS(WT)-expressing cells compared to KRAS-MUT-expressing cells. We next tested SHP2i in RAS-WT SW48 cells engineered to express KRAS-MUT from the endogenous promoter using CRISPR knock-in (**Fig. 1B**). SHP2i was less potent in suppressing MAPK signaling in KRAS(G12V) compared to KRAS(G12C)-expressing cells. MAPK signaling in KRAS(Q61R)-expressing cells was completely resistant to SHP2i, consistent with previous reports[13,15]. Similar to our experiments in Hela cells, SHP2i potently suppressed MAPK in parental, RAS-WT SW48 cells.

To further evaluate panRAS(OFF)i across KRAS(G12X) models, we tested SHP2i and SOSi in a panel of cell lines. The SOSi used was consistently less potent than the SHP2i, while both showed a suppressive effect on MAPK in G12C/A/S KRAS-MUT cells. In the KRAS(G12V)- expressing SW620 cells, basal MAPK levels were lower and minimally affected by either SHP2i or SOSi (**Fig. 1C**).

Finally, we assessed the effect of SHP2i on cell viability of various RAS(MUT) cells, along with RAS(WT) cell lines, modeling normal cells. SHP2i treatment did not preferentially suppress cell proliferation of KRAS-MUT over RAS-WT cells. Two RAS-WT lines (MRC5 and MEFs) showed substantial growth inhibition, whereas RAS-MUT cells were only marginally affected (**Fig. 1D**).

Together, these findings indicate that SHP2i, when used as monotherapy, has a low SII, as its inhibitory effects are not sufficiently selective for KRAS-MUT over RAS-WT cells. This may explain the limited clinical efficacy observed in trials assessing SHP2i for RAS-MUT cancers.

**NF1 Loss Confers Resistance to panRAS(OFF)i of KRAS(G13D) expressing cells**

Similar to KRAS(G12X) mutants, KRAS(G13D) mutations exhibit low but detectable intrinsic GTPase activity[21], suggesting a dependence on upstream RTK signaling to maintain their active state. However, previous studies have reported conflicting findings regarding the sensitivity of KRAS(G13D)-mutant cells to SHP2i. While we previously demonstrated that SHP2i is ineffective in KRAS(G13D) models[15], Mainardi et al. reported SHP2 dependence in KRAS(G13D)-mutant cells[12], and Hofmann et al. showed sensitivity of a KRAS(G13D) line (DLD-1) to SOS1 inhibition (SOS1i)[17]. As the SHP2i used in our study[15], SHP099[16] is several-fold less potent than current clinical SHP2i. To confirm that the two KRAS(G13D) models we used in our study are also insensitive to next generation SHP2i and SOSi, we tested the two KRAS(G13D) models, HCT-15 and HCT-116 used by us, with the second generation SHP2i TNO155 or the SOS1i BI-3406. In both models, MAPK inhibition was minimal (**Fig. 2A**), consistent with our previous findings[15].

The KRAS(G13D) models tested by the various groups differ in their NF1 status: DLD-1 is NF1-proficient, whereas HCT-15 and HCT-116 lack NF1 expression. This suggested that KRAS(G13D)-mutant cells require NF1 for SHP2/SOS1 dependency. In support of this idea, either SHP2i or SOS1i resulted in a modest suppression of MAPK signaling in NF1-proficient DLD-1 cells, but had no effect in NF1-deficient HCT-116 cells (**Fig. 2B**). To directly test whether NF1 loss drives insensitivity to SHP2i in the KRAS(G13D) context, we knocked down NF1 using siRNA in DLD-1 (KRAS(G13D) cells. NF1 downregulation resulted in complete resistance of MAPK inhibition by SHP2i (**Fig. 2C**), consistent with NF1 expression being required for sensitivity to SHP2i. Thus, KRAS(G13D) signaling is altered by NF1 expression, and NF1 loss diminishes sensitivity to panRAS(OFF)i. NF1 downregulation also promoted insensitivity to SHP2i in a RAS-WT model (**Fig. 2C**), suggesting that NF1 inactivation may be a general mechanism promoting insensitivity to SHP2i.

Together our findings indicate that RAS-MUT vary in their sensitivity to panRAS(OFF)i (**Fig. 2D**). RAS-MUT with increased dependence on upstream RTK/SHP2/SOS signaling have the highest sensitivity to

SHP2i (WT, KRASG12C/S/A). KRAS(G12V/D) and NF1-proficient KRAS(G13D) have modest sensitivity to SHP2i, while NF1-deficient KRAS(G13D) and RAS(Q61R/K), exhibit complete insensitivity to SHP2i.

**Combined SHP2i+MEKi suppresses MAPK activity in both normal and RAS(G12X)-mutant cells, diminishing tumor selectivity.**

MEK inhibitors (MEKi) have been assessed as a treatment for RAS-MUT tumors, however adaptive resistance through negative feedback and RAS/MAPK reactivation limits their efficacy[22-24]. Thus, combining MEKi with SHP2 inhibitors (SHP2i) has been shown by us[15] and others[11,12,25-27] to enhance MAPK pathway suppression and mitigate resistance in various RAS-MUT models.

We observed that SHP2i alone effectively inhibited ERK activity in KRAS(G12C/A/S) mutant cells, and to a lesser extent, in KRAS(G12V/D) models (**Fig. 1A, 1C**,). To assess whether the SHP2i+MEKi combination therapy could provide sustained MAPK suppression, we assessed pERK levels following short-term (2 hours) and long-term (24 hours) treatment. While SHP2i alone transiently reduced ERK activity in H1792 (KRAS(G12C)) cells, combined treatment of SHP2i (TNO155) with MEKi (Trametinib) resulted in more durable MAPK suppression (**Fig. 3A**). Similar results were observed when MEKi was combined with SOS1i (**Fig. 3A**). In KRAS(G12D) cell lines (HPAF-II, AsPC-1, and HPAC), that were less sensitive to SHP2i monotherapy, MAPK was also potently inhibited upon combined SHP2i+MEKi treatment (**Fig. 3B**). To evaluate the tumor selectivity of this approach, we tested the SHP2i+MEKi combination in isogenic HeLa cells with doxycycline (dox)-inducible expression of various KRAS(G12X). SHP2i alone more strongly inhibited pERK in RAS-WT cells than in KRAS-MUT cells. Further, combined SHP2i+MEKi resulted in comparable MAPK suppression in both WT and KRAS-MUT-expressing cells, indicating lack of selectivity for the KRAS-MUT context over RAS-WT (**Fig. 3C**).

Finally, we assessed the effect on cell viability of SHP2i and SHP2i+MEKi in a panel of normal and tumor cell lines expressing RAS-WT or KRAS(G12X), all of which were insensitive to SHP2i alone. To quantitatively compare the effects of SHP2i monotherapy versus SHP2i+MEKi treatment, we assigned viability scores based on responses to SHP2i and to SHP2i+MEKi. While KRAS(G12X) tumor cells were sensitive to the combination, RAS-WT-expressing cells (RPE-1), were also affected (**Fig. 3D**). These findings reinforce that the SHP2i+MEKi combination lacks tumor selectivity, likely explaining its poor tolerability in clinical trials and limiting its utility for treating RAS-MUT cancers.

**RAS(Q61R/K) cells are insensitive to combined SHP2i+MEKi due to feedback activation of RAS(Q61R/K) and induction of a SHP2 conformation with reduced SHP2i binding.**

We previously showed using a first generation SHP2i (SHP099) that tumor cells harboring RAS(Q61R/K) mutations exhibited complete resistance to a first generation SHP2i SHP099 alone or in combination with MEKi[15]. While RAS(Q61R/K)-mutant tumors are generally considered SHP2-independent, their resistance to dual SHP2i+MEKi therapy was unexpected, as feedback RAS activation upon MEKi treatment is thought to occur through RAS-WT and should therefore be sensitive to SHP2i. The question prompted us to further investigate the biochemical basis of RAS(Q61K/R)-driven resistance to combined SHP2i+MEKi.

First, we validated our previous result with the more potent, clinically relevant SHP2i TNO155[25], by treating SKMEL2(NRASQ61R) cells with MEKi, TNO155, a more potent second generation SHP2i[25], or the combination. Consistent with our previous report[15], MAPK rebound was fully resistant to combined SHP2i+MEKi (**Fig. 4A**). We next assessed feedback activation of RAS, by performing active RAS pulldown assays in SKMEL2 cells, which are homozygous for NRAS(Q61R). Following 24 hours of SHP2i+MEKi treatment, we observed elevated NRAS(Q61R) activity in response to the treatment (**Fig. 4B**), indicating that feedback activation of NRAS(Q61R) drives adaptive MAPK recovery.

We next investigated whether NRAS(Q61R) activation promotes a conformational change in SHP2 that affects binding of SHP2i. To test this, we used SHP2 degradation by a SHP2 PROTAC degrader[28] as a proxy for SHP2i binding to SHP2. In HEK293 cells, SHP2-PROTAC treatment significantly reduced SHP2 protein levels (**Fig. 4C**). However, when KRAS(Q61K) or NRAS(Q61R) were ectopically expressed in HEK293 cells, SHP2 degradation by SHP2 PROTAC was markedly reduced (**Fig. 4D, 4E**), indicating that RAS(Q61K/R) expression altered SHP2 conformation, impairing inhibitor accessibility. All of these findings support a mechanism of resistance to SHP2i+MEKi in RAS(Q61K/R) tumor cells, in which both feedback-driven RAS(Q61K/R) hyperactivation and structural alterations in SHP2 contribute to evasion of SHP2-targeted therapies.

**Sensitivity to any single RAS-targeted inhibitor is restricted to an overlapping subset of RAS-MUT-inhibitor sensitive tumors.**

In addition to panRAS(OFF)i (e.g., SHP2 and SOS1 inhibitors), panKRAS(OFF)-selective, as well as and panRAS(ON) inhibitors have recently been developed. To assess their SII, we determined MAPK signaling and growth inhibition in a panel of cell line models, including normal cells and KRAS(G12C)- and KRAS(G12D)-mutant cancer lines with defined sensitivity to RAS(G12C)- or RAS(G12D)-specific inhibitors (**Fig. 5A, B**). To do so, we compared the SIIs of a panRAS(OFF)i (SHP2i), a panKRAS(OFF)i (BI-2852), and a panRAS(ON)i, alongside the clinical MEKi trametinib. MEKi suppressed signaling and growth to varying degrees across these cell lines, without distinguishing between RAS(G12X) and RAS(WT), indicating a low SII. These results are consistent with clinical data demonstrating modest efficacy and dose-limiting toxicities when MEKi is used in RAS-MUT cancers[29-31]. Treatment with the panKRAS(OFF)i yielded a positive SII in RAS-MUT-sensitive models but a substantially lower SII in cell lines insensitive to RAS-MUT-specific inhibitors. Finally, treatment with the panRAS(ON)i resulted in MAPK and growth inhibition in both RAS-MUT and RAS-WT cells, showing a positive, but low SII.

Finally, we carried out a comparative analysis of our cell growth inhibition data and previously published reports of KRAS(G12C) cell lines sensitivity to KRAS(G12C)i, panRAS(OFF)i, panKRAS(OFF)i, or panRAS(ON)i. These findings revealed similar overall relative sensitivities to all RAS inhibitors (**Fig. 5C**), supporting the notion that the high antitumor efficacy of RAS inhibitors is largely restricted to the same subset of RAS-MUT cancers. Consequently, the majority of RAS-MUT tumors are predicted to show limited responsiveness to RAS inhibitors with any well characterized mechanism of action.

## Discussion

RAS-MUT-specific inhibitors have theoretically unlimited Therapeutic Index and thus can be clinically dosed at saturating concentrations. However, the Overall Response Rate (ORR) to these drugs is at best around 50%[6-8]. In addition to RAS-MUT specific inhibitors, several paralog and state-selective inhibitors have been developed as possible new therapeutic agents for RAS-MUT cancers. These include panRAS(OFF)i (e.g., SHP2i and SOS1i), panKRAS(OFF)i, sparing HRAS and NRAS (e.g., BI-2852, ERAS-4001) and panRAS(ON)i (e.g., RMC-7977, RMC-6236, ERAS-0015, GFH547). In this study, we assessed MAPK pathway and growth inhibition by such RAS inhibitors in models of RAS-MUT and RAS-WT (normal) cells and compared their Signaling Inhibition Indexes - SII (i.e. the differential inhibition of oncogenic signaling between tumor and normal cells) and relative growth inhibition. To represent normal RAS/MAPK signaling we used models of varying sensitivity to MEKi and considered

MAPK and growth inhibition by RAS signaling inhibitors in any of these models as suggesting potential on target/off tumor toxicity.

Consistent with previous reports, KRAS(G12X) mutant cells were overall sensitive to SHP2i. However, we found that KRAS(G12V/D) were less sensitive than KRAS(G12C/A/S). These results help to explain the modest results of early phase clinical trials of SHP2i in patients with KRAS(G12X) tumors[32].

We previously reported KRAS(G13D) cells to be resistant to SHP2i[15], whereas others found them to be sensitive to SHP2i[12] or SOS1i[17]. We found that differential expression of NF1 accounts for this discrepancy. KRAS(G13D) NF1-depleted cells were insensitive to SHP2i or SOS1i, whereas KRAS(G13D/NF1-proficient) cells were modestly sensitive. These data are consistent with previous reports indicating KRAS(G13D) to be sensitive to NF1-mediated hydrolysis[33] and therefore be dependent on upstream RTK/SHP2/SOS signaling (EGFR) for its activity[34,35].

Despite early preclinical findings suggesting that patients with RAS(G12X) tumors could benefit from SHP2i+MEKi therapy, clinical efficacy has been modest. We found that SHP2i+MEKi is highly potent not only in KRAS(G12X) but also in RAS-WT cells, indicating a low SII, thus explaining the modest clinical results of the combination.

RAS(Q61R) cells are resistant to SHP2i, however the basis of their resistance to combined SHP2i+MEKi[15] was not obvious. RAS(Q61R) is thought to be at the maximum of its activity and thus feedback MAPK activation should be carried through RAS-WT activation, which is sensitive to SHP2i. However, we found that RAS(Q61R) was hyperactivated in response to MAPK inhibition. This, together with SHP2 adopting a conformation with reduced SHP2i binding, as evidenced by decreased degradation by a SHP2 PROTAC, promoted resistance to SHP2i in the context of SHP2i+MEKi. As SHP2i bind the inactive, closed conformation of SHP2, RAS hyperactivation could promote a shift of the equilibrium of SHP2 towards the active conformation and thus reduce binding of SHP2i. However, further studies are required to better characterize this conformational shift of SHP2.

By assessing in parallel SII and growth inhibition by panRAS(OFF)i, panKRAS(OFF)i and panRAS(ON)i in KRAS(G12X) and RAS-WT (normal) cell models, we found that panKRAS(OFF)i show a positive SII, with minimal activity in normal cells. panRAS(ON)i are active in both RAS-MUT and RAS-WT cells, with a positive, yet narrow SII. Importantly, all paralog- and state- selective RAS inhibitors are more

potent in cell line models that are also sensitive to RAS-MUT specific inhibitors. This suggests that all RAS-targeting drugs to date are active in a similar "RAS inhibitor-sensitive" portion of tumors. These results emphasize the need for improved strategies to target the portion of RAS-MUT patients that do not respond to any of the current RAS-targeting inhibitors.

Together our findings reinforce the notion that the effectiveness of paralog- and state-selective inhibitors depends largely on specific RAS mutations and cellular context (e.g. NF1 expression), and highlight the need to integrate SII considerations into the development and clinical application of RAS-targeted therapies.

**Author Contributions**

B.B. designed and performed experiments, analyzed data and wrote the manuscript. A.O.R, B.G. X.Z., M.D. and C.A. performed experiments and analyzed data. S.A.A. designed experiments and analyzed data. S.W. developed and contributed the SHP2 PROTAC and analyzed data. P.I.P. conceived the study, supervised and coordinated research, analyzed data and wrote the manuscript.

**Competing Interests**

P.I.P reports research funding to his institution by Verastem Oncology and Enliven Therapeutics and consulting fees from Nuvalent Inc, Blueprint Medicines, Belharra Therapeutics and Fore-Bio.

**References**


1. Young, A., Lyons, J., Miller, A.L., Phan, V.T., Alarcon, I.R., and McCormick, F. (2009). Ras signaling and therapies. Advances in cancer research *102*, 1-17. 10.1016/S0065-230X(09)02001-6.
2. Baines, A.T., Xu, D., and Der, C.J. (2011). Inhibition of Ras for cancer treatment: the search continues. Future medicinal chemistry *3*, 1787-1808. 10.4155/fmc.11.121.
3. Moore, A.R., Rosenberg, S.C., McCormick, F., and Malek, S. (2021). RAS-targeted therapies. Nature reviews. Drug discovery. 10.1038/s41573-021-00220-6.
4. Cox, A.D., Fesik, S.W., Kimmelman, A.C., Luo, J., and Der, C.J. (2014). Drugging the undruggable RAS: Mission possible? Nature reviews. Drug discovery *13*, 828-851. 10.1038/nrd4389.
5. Ostrem, J.M., Peters, U., Sos, M.L., Wells, J.A., and Shokat, K.M. (2013). K-Ras(G12C) inhibitors allosterically control GTP affinity and effector interactions. Nature *503*, 548-551. 10.1038/nature12796.
6. Hong, D.S., Fakih, M.G., Strickler, J.H., Desai, J., Durm, G.A., Shapiro, G.I., Falchook, G.S., Price, T.J., Sacher, A., Denlinger, C.S., et al. (2020). KRAS(G12C) Inhibition with Sotorasib in

Advanced Solid Tumors. The New England journal of medicine *383*, 1207-1217. 10.1056/NEJMoa1917239.
7. Skoulidis, F., Li, B.T., Dy, G.K., Price, T.J., Falchook, G.S., Wolf, J., Italiano, A., Schuler, M., Borghaei, H., Barlesi, F., et al. (2021). Sotorasib for Lung Cancers with KRAS p.G12C Mutation. The New England journal of medicine *384*, 2371-2381. 10.1056/NEJMoa2103695.
8. Janne, P.A., Riely, G.J., Gadgeel, S.M., Heist, R.S., Ou, S.I., Pacheco, J.M., Johnson, M.L., Sabari, J.K., Leventakos, K., Yau, E., et al. (2022). Adagrasib in Non-Small-Cell Lung Cancer Harboring a KRAS(G12C) Mutation. The New England journal of medicine *387*, 120-131. 10.1056/NEJMoa2204619.
9. Yaeger, R., Weiss, J., Pelster, M.S., Spira, A.I., Barve, M., Ou, S.I., Leal, T.A., Bekaii-Saab, T.S., Paweletz, C.P., Heavey, G.A., et al. (2023). Adagrasib with or without Cetuximab in Colorectal Cancer with Mutated KRAS G12C. The New England journal of medicine *388*, 44-54. 10.1056/NEJMoa2212419.
10. The KRAS(G12D) inhibitor MRTX1133 elucidates KRAS-mediated oncogenesis. (2022). Nature medicine *28*, 2017-2018. 10.1038/s41591-022-02008-6.
11. Fedele, C., Ran, H., Diskin, B., Wei, W., Jen, J., Geer, M.J., Araki, K., Ozerdem, U., Simeone, D.M., Miller, G., et al. (2018). SHP2 Inhibition Prevents Adaptive Resistance to MEK Inhibitors in Multiple Cancer Models. Cancer discovery. 10.1158/2159-8290.CD-18-0444.
12. Mainardi, S., Mulero-Sanchez, A., Prahallad, A., Germano, G., Bosma, A., Krimpenfort, P., Lieftink, C., Steinberg, J.D., de Wit, N., Goncalves-Ribeiro, S., et al. (2018). SHP2 is required for growth of KRAS-mutant non-small-cell lung cancer in vivo. Nature medicine. 10.1038/s41591-018-0023-9.
13. Nichols, R.J., Haderk, F., Stahlhut, C., Schulze, C.J., Hemmati, G., Wildes, D., Tzitzilonis, C., Mordec, K., Marquez, A., Romero, J., et al. (2018). RAS nucleotide cycling underlies the SHP2 phosphatase dependence of mutant BRAF-, NF1- and RAS-driven cancers. Nat Cell Biol *20*, 1064-1073. 10.1038/s41556-018-0169-1.
14. Ruess, D.A., Heynen, G.J., Ciecielski, K.J., Ai, J., Berninger, A., Kabacaoglu, D., Gorgulu, K., Dantes, Z., Wormann, S.M., Diakopoulos, K.N., et al. (2018). Mutant KRAS-driven cancers depend on PTPN11/SHP2 phosphatase. Nature medicine. 10.1038/s41591-018-0024-8.
15. Ahmed, T.A., Adamopoulos, C., Karoulia, Z., Wu, X., Sachidanandam, R., Aaronson, S.A., and Poulikakos, P.I. (2019). SHP2 Drives Adaptive Resistance to ERK Signaling Inhibition in Molecularly Defined Subsets of ERK-Dependent Tumors. Cell Rep *26*, 65-78 e65. 10.1016/j.celrep.2018.12.013.
16. Chen, Y.N., LaMarche, M.J., Chan, H.M., Fekkes, P., Garcia-Fortanet, J., Acker, M.G., Antonakos, B., Chen, C.H., Chen, Z., Cooke, V.G., et al. (2016). Allosteric inhibition of SHP2 phosphatase inhibits cancers driven by receptor tyrosine kinases. Nature *535*, 148-152. 10.1038/nature18621.
17. Hofmann, M.H., Gmachl, M., Ramharter, J., Savarese, F., Gerlach, D., Marszalek, J.R., Sanderson, M.P., Kessler, D., Trapani, F., Arnhof, H., et al. (2021). BI-3406, a Potent and Selective SOS1-KRAS Interaction Inhibitor, Is Effective in KRAS-Driven Cancers through Combined MEK Inhibition. Cancer discovery *11*, 142-157. 10.1158/2159-8290.CD-20-0142.
18. Kim, D., Herdeis, L., Rudolph, D., Zhao, Y., Bottcher, J., Vides, A., Ayala-Santos, C.I., Pourfarjam, Y., Cuevas-Navarro, A., Xue, J.Y., et al. (2023). Pan-KRAS inhibitor disables oncogenic signalling and tumour growth. Nature *619*, 160-166. 10.1038/s41586-023-06123-3.
19. Holderfield, M., Lee, B.J., Jiang, J., Tomlinson, A., Seamon, K.J., Mira, A., Patrucco, E., Goodhart, G., Dilly, J., Gindin, Y., et al. (2024). Concurrent inhibition of oncogenic and wild-type RAS-GTP for cancer therapy. Nature. 10.1038/s41586-024-07205-6.

20. Wasko, U.N., Jiang, J., Dalton, T.C., Curiel-Garcia, A., Edwards, A.C., Wang, Y., Lee, B., Orlen, M., Tian, S., Stalnecker, C.A., et al. (2024). Tumor-selective activity of RAS-GTP inhibition in pancreatic cancer. Nature. 10.1038/s41586-024-07379-z.
21. Hunter, J.C., Manandhar, A., Carrasco, M.A., Gurbani, D., Gondi, S., and Westover, K.D. (2015). Biochemical and Structural Analysis of Common Cancer-Associated KRAS Mutations. Mol Cancer Res *13*, 1325-1335. 10.1158/1541-7786.MCR-15-0203.
22. Samatar, A.A., and Poulikakos, P.I. (2014). Targeting RAS-ERK signalling in cancer: promises and challenges. Nature reviews. Drug discovery *13*, 928-942. 10.1038/nrd4281.
23. Sun, C., and Bernards, R. (2014). Feedback and redundancy in receptor tyrosine kinase signaling: relevance to cancer therapies. Trends Biochem Sci *39*, 465-474. 10.1016/j.tibs.2014.08.010.
24. Duncan, J.S., Whittle, M.C., Nakamura, K., Abell, A.N., Midland, A.A., Zawistowski, J.S., Johnson, N.L., Granger, D.A., Jordan, N.V., Darr, D.B., et al. (2012). Dynamic reprogramming of the kinome in response to targeted MEK inhibition in triple-negative breast cancer. Cell *149*, 307-321. 10.1016/j.cell.2012.02.053.
25. Liu, C., Lu, H., Wang, H., Loo, A., Zhang, X., Yang, G., Kowal, C., Delach, S., Wang, Y., Goldoni, S., et al. (2021). Combinations with Allosteric SHP2 Inhibitor TNO155 to Block Receptor Tyrosine Kinase Signaling. Clinical cancer research : an official journal of the American Association for Cancer Research *27*, 342-354. 10.1158/1078-0432.CCR-20-2718.
26. Lu, H., Liu, C., Velazquez, R., Wang, H., Dunkl, L.M., Kazic-Legueux, M., Haberkorn, A., Billy, E., Manchado, E., Brachmann, S.M., et al. (2019). SHP2 Inhibition Overcomes RTK-Mediated Pathway Reactivation in KRAS-Mutant Tumors Treated with MEK Inhibitors. Molecular cancer therapeutics *18*, 1323-1334. 10.1158/1535-7163.MCT-18-0852.
27. Wong, G.S., Zhou, J., Liu, J.B., Wu, Z., Xu, X., Li, T., Xu, D., Schumacher, S.E., Puschhof, J., McFarland, J., et al. (2018). Targeting wild-type KRAS-amplified gastroesophageal cancer through combined MEK and SHP2 inhibition. Nature medicine. 10.1038/s41591-018-0022-x.
28. Wang, M., Lu, J., Wang, M., Yang, C.Y., and Wang, S. (2020). Discovery of SHP2-D26 as a First, Potent, and Effective PROTAC Degrader of SHP2 Protein. Journal of medicinal chemistry *63*, 7510-7528. 10.1021/acs.jmedchem.0c00471.
29. Janne, P.A., Shaw, A.T., Pereira, J.R., Jeannin, G., Vansteenkiste, J., Barrios, C., Franke, F.A., Grinsted, L., Zazulina, V., Smith, P., et al. (2013). Selumetinib plus docetaxel for KRAS-mutant advanced non-small-cell lung cancer: a randomised, multicentre, placebo-controlled, phase 2 study. The lancet oncology *14*, 38-47. 10.1016/S1470-2045(12)70489-8.
30. Blumenschein, G.R., Jr., Smit, E.F., Planchard, D., Kim, D.W., Cadranel, J., De Pas, T., Dunphy, F., Udud, K., Ahn, M.J., Hanna, N.H., et al. (2015). A randomized phase II study of the MEK1/MEK2 inhibitor trametinib (GSK1120212) compared with docetaxel in KRAS-mutant advanced non-small-cell lung cancer (NSCLC)dagger. Ann Oncol *26*, 894-901. 10.1093/annonc/mdv072.
31. Ascierto, P.A., Schadendorf, D., Berking, C., Agarwala, S.S., van Herpen, C.M., Queirolo, P., Blank, C.U., Hauschild, A., Beck, J.T., St-Pierre, A., et al. (2013). MEK162 for patients with advanced melanoma harbouring NRAS or Val600 BRAF mutations: a non-randomised, open-label phase 2 study. The lancet oncology *14*, 249-256. 10.1016/S1470-2045(13)70024-X.
32. . https://www.jto.org/article/S1556-0864(19)33761-X/fulltext.
33. Rabara, D., Tran, T.H., Dharmaiah, S., Stephens, R.M., McCormick, F., Simanshu, D.K., and Holderfield, M. (2019). KRAS G13D sensitivity to neurofibromin-mediated GTP hydrolysis. Proceedings of the National Academy of Sciences of the United States of America *116*, 22122-22131. 10.1073/pnas.1908353116.

34. McFall, T., and Stites, E.C. (2020). A mechanism for the response of KRAS(G13D) expressing colorectal cancers to EGFR inhibitors. Mol Cell Oncol *7*, 1701914. 10.1080/23723556.2019.1701914.
35. McFall, T., and Stites, E.C. (2021). Identification of RAS mutant biomarkers for EGFR inhibitor sensitivity using a systems biochemical approach. Cell Rep *37*, 110096. 10.1016/j.celrep.2021.110096.

## Material and Methods

### *Compounds*

TNO155 (S8987) and Trametinib (S2673) were obtained from Selleckchem. MRTX-0902 (HY-145926) was obtained from Medchem Express. BI-2865 (C-1443) was obtained from Chemgood. SHP2 degrader (SHP2-D26) was developed and contributed by Shaomeng Wang (University of Michigan). Compounds were dissolved in DMSO to yield 10 mmol/L stock.

### *Cell lines*

H358, Calu-1, H1792, MIAPaCa-2, H1573, A549, SW620, HPAC, HPAF-II, AsPC.1, PANC.1, SW1990, HCT-15, HCT-116, DLD-1, Calu-6, SK-MEL-2, and HEK293T cell lines were purchased from American Type Culture Collection. HEK293 cell line was purchased from Life Technologies. Isogenic SW48 cells were obtained from Horizon Discovery. HeLa cells were kindly provided by Ramon Parsons (Icahn School of Medicine at Mount Sinai). RPE.1, AC16, HCT-E, and MRC5 cell lines were a gift from Anthony Faber. MEF cell lines has been described previously (7) All the cells used in the study were maintained in a humidified incubator at 37°C with 5% CO2 and cultured in RPMI 1640 (ThermoFisher, 11-875-119) or DMEM (ThermoFisher, 10313-039) supplemented with 10% FBS (Biowest, S1680), 2 mmol/L glutamine (ThermoFisher, 25-030-164), and 100 IU/mL penicillin/streptomycin (ThermoFisher, 15-140-163) and were passaged from three to five times. Cell lines were authenticated by LabCorp using short tandem repeat DNA profiling and regularly tested negatively for Mycoplasma using the Venor GeM Mycoplasma Detection Kit (Sigma).

### *Plasmids and transfections*

pMEVHA-KRAS2A-WT was purchased from Biomyx (P1020). NRAS was subcloned using pMEV as a backbone. N-terminal HA-tagged KRAS was subcloned into pTRI-BlasticidinS plasmid (From Yuki Otsuka). KRAS (G12C, G12D, G12A, G12S, G12V, Q61K) and NRAS (Q61R) activating mutants were

generated with the QuikChange II XL Site-Directed Mutagenesis Kit (Agilent, 200522). Transfections were carried out using Lipofectamine 2000 (ThermoFisher, 11668019).

***NF1 gene silencing***

DLD-1 cells and HeLa cells were transfected with 600 pmol of ON-TARGETplus human NF1 siRNA (Horizon Discovery) or ON-TARGETplus non-targeting control pool (Horizon Discovery) using Lipofectamine RNAiMAX transfection reagent (Invitrogen) following manufacturer's instructions. 24 hr later, cells were treated with the indicated drugs, and NF1 levels were evaluated by Western blot as previously described.

***Lentivirus transduction and doxycycline-inducible stable cell line generation***

Lentivirus was produced by transfecting HEK293T cells with the pTRI-BlaS transfer plasmid containing various KRAS variants (KRAS (WT, G12C, G12D, G12S, G12A, G12V, Q61K), the packaging vector psPAX2 (Addgene), and envelope vector pMD2.G (Addgene) a 5:4:1 ratio using Lipofectamine 2000 (ThermoFisher, 11668019). The viral supernatant was collected 72 hours after transfection and filtered through a 0.45-µm filter unit (MilliporeSigma, SLHPR33RS). After 24 h, HEK293T medium was replaced with fresh medium, and 48 h after the co-transfection, the medium containing lentiviral particles was collected, filtered, and used to infect HeLa cells after the addition of 10 µg/mL polybrene (Sigma-Aldrich). HeLa cells were incubated overnight at 37°C prior to the removal of viral particles and the addition of fresh media. Transduced cells were then selected for by culturing in the presence of 3 µg/ml Blasticidin (Invivogen, ant-bl-05) for approximately 10 days. Cells were cultured in the presence of 50-600 ng/ml doxycycline for 24 hours prior to use in experiments.

***Western blot and active RAS pull-down***

Cells were washed with PBS and lysed on ice for 5 minutes in NP40 buffer (50 mmol/L Tris pH 7.5, 1% NP40, 150 mmol/L NaCl, 10% Glycerol 1 mmol/L EDTA) supplemented with protease (Roche, 11873580001) and phosphatase inhibitors (Roche, 4906837001). Lysates were centrifuged at 15,000 rpm for 10 minutes, and the protein concentration was quantified using BCA (ThermoFisher, 23221, 23224). Proteins were separated by NuPAGE and 4% to 12% Bis Tris Gel (Invitrogen, NP0321BOX), and they were immunoblotted and transferred to nitrocellulose membranes (GE Healthcare, 45-004-006) according to standard protocols. Membranes were immunoblotted overnight with antibodies against:

pMEK1/2$^{Ser217/22}$ (9154), MEK1 (2352), pERK1/2$^{Thr202/Tyr204}$ (4370) from Cell Signaling; SHP2 (sc-7384) and NRAS (sc-31) from Santa Cruz Biotechnology; pSHP2$^{Y542}$ from abcam (ab62322); NF1 from Invitrogen (PA5-103218), hemagglutin (HA) from Biolegend (901501); V5 from ThermoFisher (R960-25); KRAS from (Proteintech, 12063-1-AP). The next day, membranes were probed with anti-rabbit IgG (Cell Signaling, 7074) or anti-mouse IgG secondary antibody (Cell Signaling, 7076), and chemiluminescent signals were detected on X-ray films.

RAS pull-down kit (ThermoFisher, 16117) was used to determine levels of RAS-GTP, according to the manufacturer's protocol. RAS was detected by western blot using either an antibody for KRAS (Santa Cruz Biotechnology, sc-30), or pan-RAS antibody provided with the kit.

***Cellular viability assay***

Cells were plated at a density of 0.5-1 x $10^3$ cells per well in 96-well plates (Corning$^{TM}$, 3595). The next day, cells were treated with inhibitors as indicated in regular growth media for 6 days. 10 µl of Cell Counting Kit-8 (Dojindo Molecular Technologies, Inc., CK04) was added, and the cells were incubated at 37 °C for 2.5 hours. Cell viability was then determined by measuring the absorbance at 450 nm using a plate reader. Dose response curves and GI50 values were calculated using log-transformed, normalized data in Graphpad Prism 10.4.1.

**Figure legends**

**Figure 1. KRAS(G12X)-expressing cells exhibit differential sensitivity to panRAS(OFF)i. (A)** Parental and Doxycycline-inducible KRAS variant HeLa cells were treated for 24 hours with increasing concentrations of doxycycline (50-600ng/mL), followed by treatment for 2 hours with SHP2 inhibitor TNO155 (0.1 or 1µM). SHP2 and MAPK pathway activation was monitored by immunoblotting. **(B)** Parental and isogenic SW48 cells expressing different KRAS mutants were treated for 2 hours with SHP2 inhibitor TNO155 (0.1, 0.3 and 1 µM). MAPK pathway activation was monitored by immunoblotting. **(C)** A panel of KRAS mutant cell lines was treated for 2 hours with either SHP2 inhibitor TNO155 (5 µM) or SOS1 inhibitor BI-3406 (10 µM). MAPK pathway activation was assessed by monitoring pERK levels via immunoblotting. **(D)** The indicated cell lines expressing either KRAS (WT) or different KRAS mutants were treated with SHP2 inhibitor TNO155 (2 µM) for 6 days. Cell viability inhibition was monitored and presented as mean ± SEM from two independent experiments (n=2).

**Figure 2. NF1 Loss Confers Resistance to panRAS(OFF)i in KRAS(G13D) expressing cells (A)** KRAS (G13D)-mutant cell lines HCT-15 and HCT-116 were treated for 2 hours with SHP2 inhibitor TNO155 (5 μM) or SOS1 inhibitor BI-3406 (10 μM). MAPK pathway activity was assessed by immunoblotting. **(B)** KRAS (G13D)-mutant cell lines DLD-1 (NF1-proficient) and HCT-116 (NF1-deficient) were treated for 2 or 24 hours with increasing concentration of SHP2 inhibitor TNO155 (0.5, 1, 2, 4, 8 μM) or SOS1 inhibitor MRTX-0902 (0.5, 1, 2, 4, 8 μM). SHP2 and MAPK pathway activation were monitored by immunoblotting, respectively indicated by $pSHP2^{Y542}$ and pMEK/pERK. **(C)** NF1 expression was transiently knocked-down in DLD-1 and HeLa, followed by treatment with SHP2i TNO155 (8 μM for DLD-1 and 4 μM for HeLa) for 2 hours. SHP2 and MAPK pathway activation were monitored by immunoblotting, respectively indicated by $pSHP2^{Y542}$ and pMEK/pERK. **(D)** Schematic model depicting the ranking of KRAS (WT) and mutant variants based on their sensitivity to SHP2 inhibition, which correlates with the contribution of receptor tyrosine kinase (RTK)-mediated MAPK pathway activation. This figure was created in BioRender. Baars, B. (2025) https://BioRender.com/y27u304.

**Figure 3. SHP2i+MEKi combination suppresses MAPK activity in both normal and RAS(G12X)-mutant cells, diminishing tumor selectivity.** (**A)** RAS (G12X) mutant cell lines were treated for 2 or 24 hours with MEK inhibitor Trametinib (5 nM), SHP2 inhibitor TNO155 (concentration adjusted for each cell line), SOS1 inhibitor BI-3406 (10 μM), or the combinations of MEKi+SHP2i or MEKi+SOS1. SHP2 and MAPK pathway activation were monitored by immunoblotting, respectively indicated by $pSHP2^{Y542}$ and pERK. H1792 and KRAS (G12D)-mutant (HPAF-II, AsPC-1, HPAC) cell lines were treated with 5μM or 2μM of SHP2 inhibitor TNO155, respectively. **(B)** Doxycycline-inducible KRAS variant HeLa cells were treated with increasing concentrations of doxycycline (50-600ng/mL) for 24 hours, followed by treatment with MEK inhibitor Trametinib (5 nM), SHP2 inhibitor TNO155 (2 μM), or the combination of MEKi+SHP2i. SHP2 and MAPK pathway activation were monitored by immunoblotting, respectively indicated by $pSHP2^{Y542}$ and pERK. **(C)** A panel of cell line expressing either KRAS (WT) or different KRAS mutants was treated for 6 days with SHP2 inhibitor TNO155 (5 μM) or MEK inhibitor Trametinib (3nM). Cell viability inhibition was assessed and presented as a score assigned to each cell line, representing the ratio between the relative viability after SHP2i treatment and the relative viability after combination. Data are represented as mean values ± SEM, n=3 experimental replicates.

**Figure 4. RAS(Q61R/K) cells are insensitive to combined SHP2i+MEKi due to feedback activation of RAS(Q61R/K) and induction of a SHP2 conformation with reduced binding to SHP2i. (A)** NRAS (Q61R) mutant cell line SKMEL2 was treated for 2 or 24 hours with either MEK inhibitor Trametinib (5 nM), SHP2 inhibitor TNO155 (5μM), or the combination MEKi+SHP2i. SHP2 and MAPK pathway activation were monitored by immunoblotting, respectively indicated by pSHP2$^{Y542}$ and pERK. **(B)** SKMEL2 cells were treated for 2 hours with SHP2 inhibitor TNO155 (5 μM) combined with MEK inhibitor Trametinib (5 nM) . The level of activated RAS (RAS-GTP) and activated NRAS (NRAS-GTP) were assessed using a RAS-pull down assay. **(C)** Left: Schematic representation of PROTAC-mediated targeted degradation of SHP2. Right: HEK293 cells were treated with increasing concentrations of SHP2-PROTAC SHP2-D26 (0.1, 0.3, 1, 3 μM) for 6 or 24 hours. SHP2 degradation and MAPK pathway activation were assessed by immunoblotting, respectively indicated by SHP2 and pERK. **(D)** HEK293 cells ectopically expressing HA-tagged KRAS (Q61K) or NRAS (Q61R) were treated for 24 hours with increasing concentrations of SHP2-D26 (0.1, 0.3, 1, 3 μM). SHP2 degradation and MAPK pathway activation were assessed by immunoblotting, respectively indicated by SHP2 and pERK. (E) HEK293 cells were transfected with varying amounts (0.25, 0.5, 1, 2 μg) of HA-tagged KRAS (Q61K) or NRAS (Q61R), followed by treatment with increasing concentrations of SHP2-D26 (0.5 μM) for 24 hours. SHP2 degradation and MAPK pathway activation were assessed by immunoblotting, respectively indicated by SHP2 and pERK.

**Figure 5. Sensitivity to any single RAS-targeted inhibitor is restricted to the subset of RAS-MUT-inhibitor sensitive tumors.** (**A**) The indicated RAS (WT), KRAS (G12C) and KRAS (G12D)-mutant cell lines were treated with increasing concentrations of panRAS(OFF)i SHP2i (0-10 μM), panKRAS(OFF)i BI-2865 (0-20 μM), and panRAS(ON)i (0-100 nM) (A) After 4 or 24 hours of treatment, MAPK pathway activation were assessed by immunoblotting, indicated by pERK. (**B**) Cell viability inhibition was assessed after 6 days of treatment. Dose-response curves were generated (top) and for each compound, GI50 for each cell line was generated and shown in the bar plot (bottom). Data are presented as mean ± SEM from three experimental replicates (n=3). (**C**) Comparative analysis of inhibitor sensitivity incorporating cell viability data from other studies. Four KRAS(G12C)-mutant cell lines that were used in our experiments and other studies were ranked based on their sensitivity to indicated inhibitors (most sensitive = 1, least sensitive = 4). Heat map was created in BioRender. Baars, B. (2025) https://BioRender.com/b56z167.

# Fig. 1.

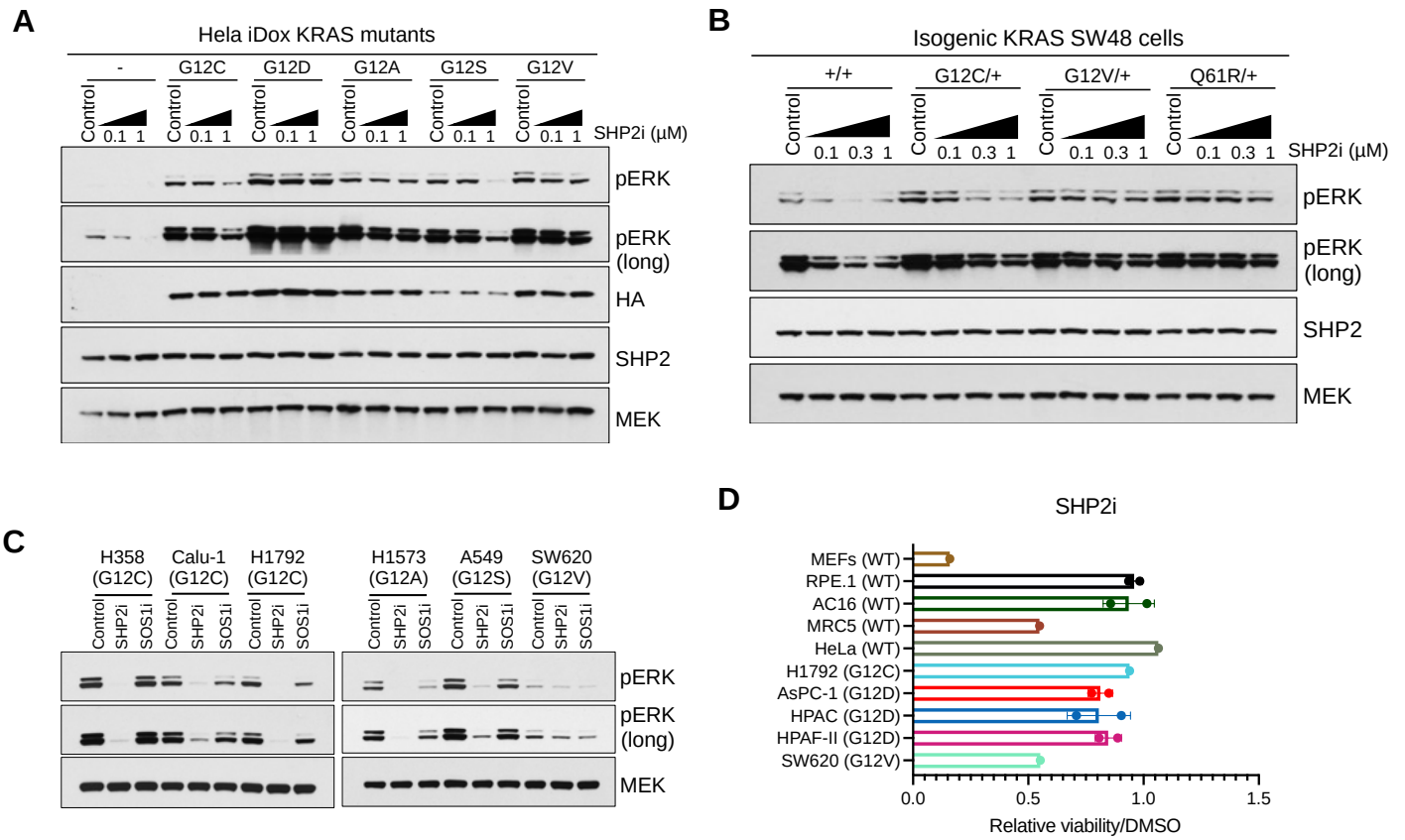
A
Hela iDox KRAS mutants
-
G12C
G12D
G12A
G12S
G12V
Control
0.1 1
SHP2i (μM)
pERK
pERK (long)
HA
SHP2
MEK
B
Isogenic KRAS SW48 cells
+/+
G12C/+
G12V/+
Q61R/+
Control
0.1 0.3 1
SHP2i (μM)
pERK
pERK (long)
SHP2
MEK
C
H358 (G12C)
Calu-1 (G12C)
H1792 (G12C)
H1573 (G12A)
A549 (G12S)
SW620 (G12V)
Control
SHP2i
SOS1i
pERK
pERK (long)
MEK
D
SHP2i
MEFs (WT)
RPE.1 (WT)
AC16 (WT)
MRC5 (WT)
HeLa (WT)
H1792 (G12C)
AsPC-1 (G12D)
HPAC (G12D)
HPAF-II (G12D)
SW620 (G12V)
0.0
0.5
1.0
1.5
Relative viability/DMSO

# Fig. 2.

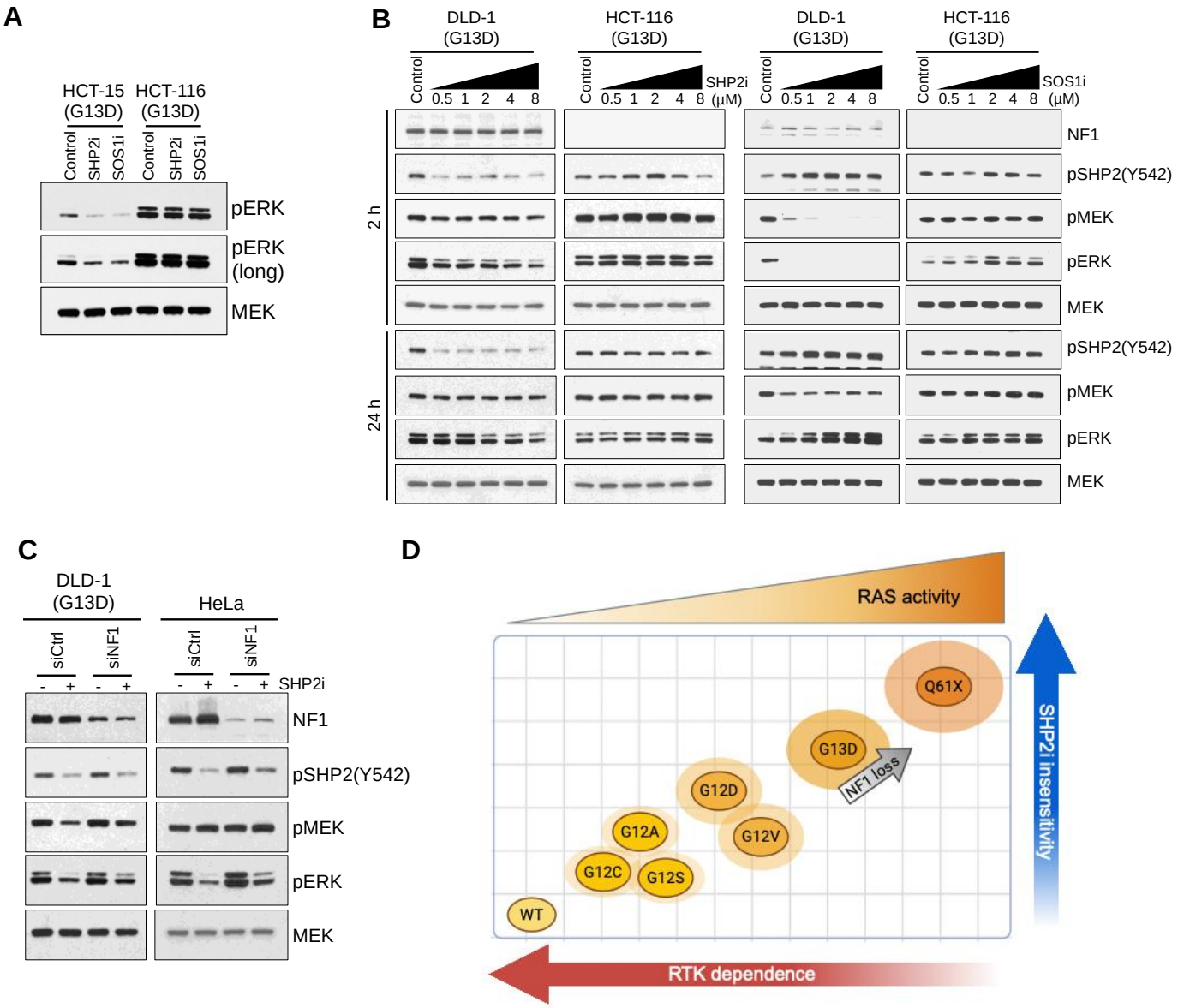
A
HCT-15 (G13D)
HCT-116 (G13D)
Control
SHP2i
SOS1i
pERK
pERK (long)
MEK
B
DLD-1 (G13D)
HCT-116 (G13D)
Control
0.5 1 2 4 8
SHP2i (μM)
SOS1i (μM)
2 h
24 h
NF1
pSHP2(Y542)
pMEK
pERK
MEK
C
DLD-1 (G13D)
HeLa
siCtrl
siNF1
SHP2i
NF1
pSHP2(Y542)
pMEK
pERK
MEK
D
RAS activity
SHP2i insensitivity
RTK dependence
Q61X
G13D
NF1 loss
G12D
G12A
G12V
G12C
G12S
WT

# Fig. 3.

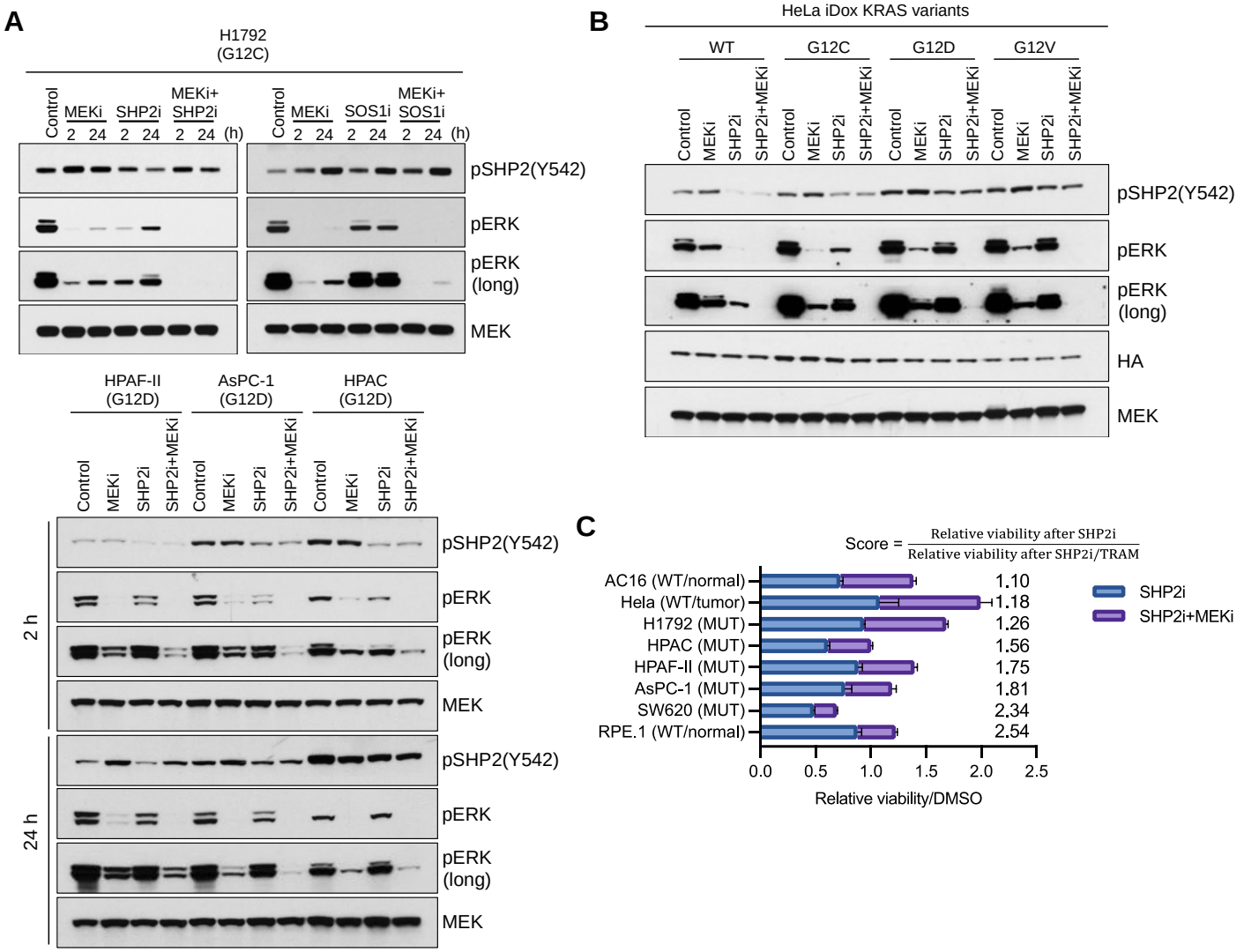
A
H1792
(G12C)
Control
MEKi
SHP2i
MEKi+
SHP2i
SOS1i
MEKi+
SOS1i
2 24 2 24 2 24 (h)
pSHP2(Y542)
pERK
pERK
(long)
MEK
HPAF-II
(G12D)
AsPC-1
(G12D)
HPAC
(G12D)
SHP2i+MEKi
2 h
24 h
B
HeLa iDox KRAS variants
WT
G12C
G12D
G12V
HA
C
Score = Relative viability after SHP2i / Relative viability after SHP2i/TRAM
AC16 (WT/normal)
Hela (WT/tumor)
H1792 (MUT)
HPAC (MUT)
HPAF-II (MUT)
AsPC-1 (MUT)
SW620 (MUT)
RPE.1 (WT/normal)
1.10
1.18
1.26
1.56
1.75
1.81
2.34
2.54
0.0
0.5
1.0
1.5
2.0
2.5
Relative viability/DMSO
SHP2i
SHP2i+MEKi

# Fig. 4.

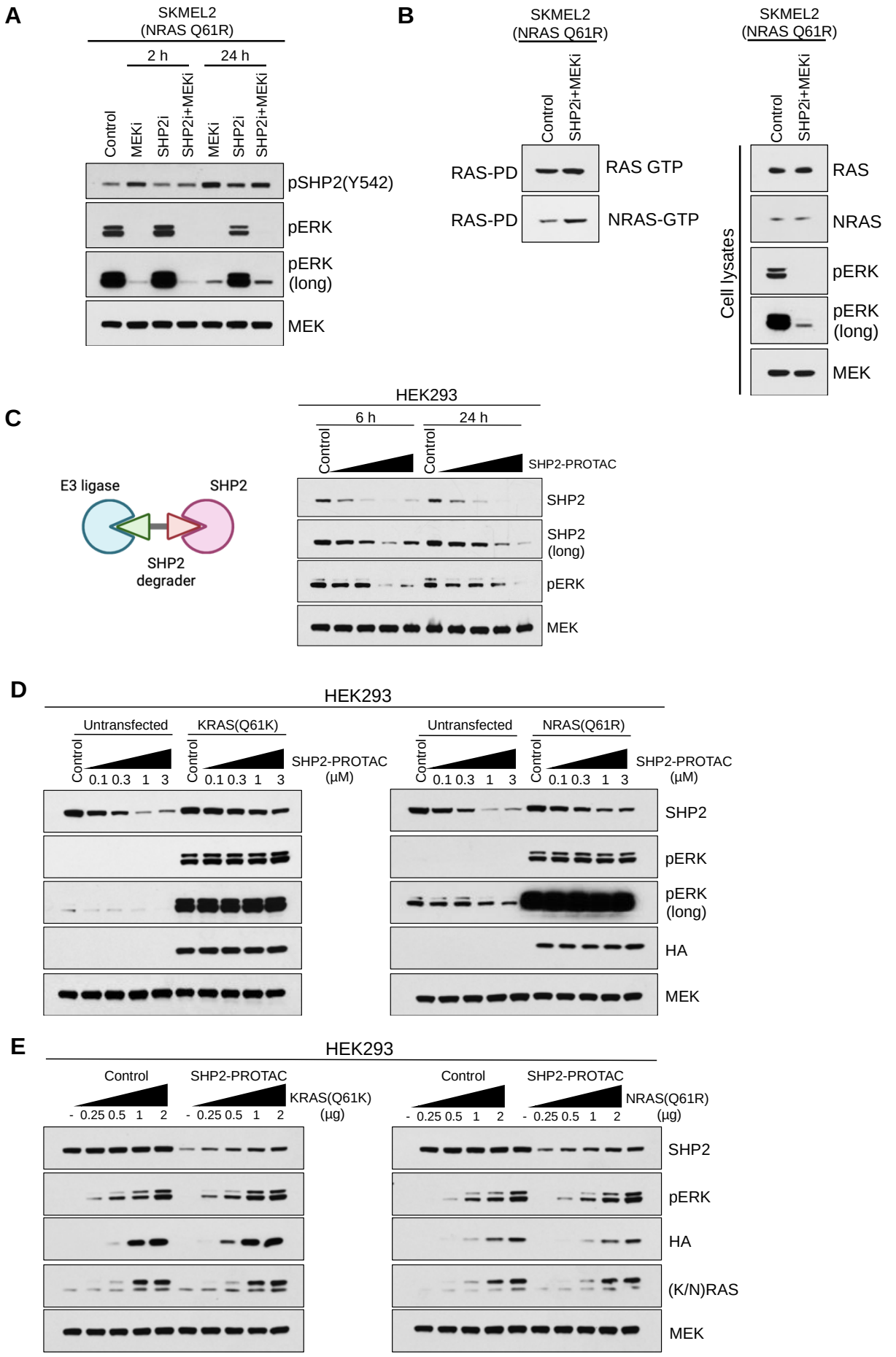
A
SKMEL2
(NRAS Q61R)
2 h
24 h
Control
MEKi
SHP2i
SHP2i+MEKi
MEKi
SHP2i
SHP2i+MEKi
pSHP2(Y542)
pERK
pERK
(long)
MEK
B
SKMEL2
(NRAS Q61R)
Control
SHP2i+MEKi
RAS-PD
RAS GTP
RAS-PD
NRAS-GTP
SKMEL2
(NRAS Q61R)
Control
SHP2i+MEKi
Cell lysates
RAS
NRAS
pERK
pERK
(long)
MEK
C
E3 ligase
SHP2
SHP2
degrader
HEK293
6 h
24 h
Control
Control
SHP2-PROTAC
SHP2
SHP2
(long)
pERK
MEK
D
HEK293
Untransfected
KRAS(Q61K)
Untransfected
NRAS(Q61R)
Control
0.1 0.3 1 3
SHP2-PROTAC
(μM)
SHP2
pERK
pERK
(long)
HA
MEK
E
HEK293
Control
SHP2-PROTAC
KRAS(Q61K)
(μg)
- 0.25 0.5 1 2
NRAS(Q61R)
(μg)
SHP2
pERK
HA
(K/N)RAS
MEK

# Fig. 5.

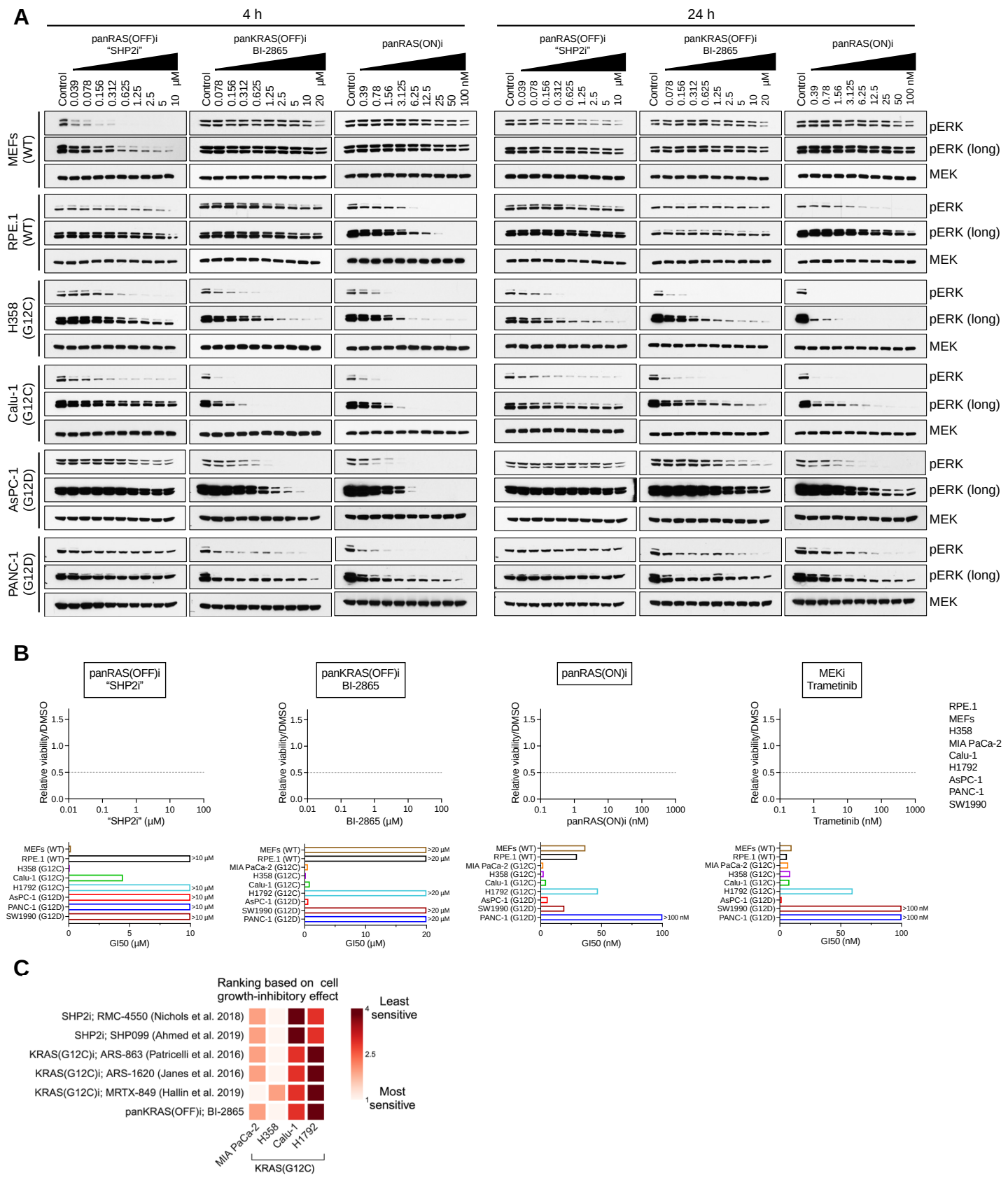
A
4 h
24 h
panRAS(OFF)i "SHP2i"
panKRAS(OFF)i BI-2865
panRAS(ON)i
Control 0.039 0.078 0.156 0.312 0.625 1.25 2.5 5 10 μM
Control 0.078 0.156 0.312 0.625 1.25 2.5 5 10 20 μM
Control 0.39 0.78 1.56 3.125 6.25 12.5 25 50 100 nM
Control 0.039 0.078 0.156 0.312 0.625 1.25 2.5 5 10 μM
Control 0.078 0.156 0.312 0.625 1.25 2.5 5 10 20 μM
Control 0.39 0.78 1.56 3.125 6.25 12.5 25 50 100 nM
MEFs (WT)
RPE.1 (WT)
H358 (G12C)
Calu-1 (G12C)
AsPC-1 (G12D)
PANC-1 (G12D)
pERK
pERK (long)
MEK
B
panRAS(OFF)i "SHP2i"
panKRAS(OFF)i BI-2865
panRAS(ON)i
MEKi Trametinib
Relative viability/DMSO
"SHP2i" (μM)
BI-2865 (μM)
panRAS(ON)i (nM)
Trametinib (nM)
RPE.1
MEFs
H358
MIA PaCa-2
Calu-1
H1792
AsPC-1
PANC-1
SW1990
GI50 (μM)
GI50 (nM)
C
Ranking based on cell growth-inhibitory effect
SHP2i; RMC-4550 (Nichols et al. 2018)
SHP2i; SHP099 (Ahmed et al. 2019)
KRAS(G12C)i; ARS-863 (Patricelli et al. 2016)
KRAS(G12C)i; ARS-1620 (Janes et al. 2016)
KRAS(G12C)i; MRTX-849 (Hallin et al. 2019)
panKRAS(OFF)i; BI-2865
MIA PaCa-2
H358
Calu-1
H1792
KRAS(G12C)
Least sensitive
Most sensitive